AUTHOR QUERY FORM

ELSEVIER	**Journal: JCOMA** **Article Number: 4129**	**Please e-mail your responses and any corrections to:** **E-mail: corrections.esch@elsevier.sps.co.in**

Dear Author,

Please check your proof carefully and mark all corrections at the appropriate place in the proof (e.g., by using on-screen annotation in the PDF file) or compile them in a separate list. Note: if you opt to annotate the file with software other than Adobe Reader then please also highlight the appropriate place in the PDF file. To ensure fast publication of your paper please return your corrections within 48 hours.

For correction or revision of any artwork, please consult http://www.elsevier.com/artworkinstructions.

Any queries or remarks that have arisen during the processing of your manuscript are listed below and highlighted by flags in the proof. Click on the 'Q' link to go to the location in the proof.

Location in article	Query / Remark: **click on the Q link to go** **Please insert your reply or correction at the corresponding line in the proof**
Q1	Your article is registered as a regular item and is being processed for inclusion in a regular issue of the journal. If this is NOT correct and your article belongs to a Special Issue/Collection please contact c.emmanuel@elsevier.com immediately prior to returning your corrections.
Q2	Please confirm that given name(s) and surname(s) have been identified correctly.
Q3	The affiliation `b' has been split into two different affiliations. Please check, and correct if necessary.
Q4	Keywords `A. Nanocomposites' and `E. Electrospinning' do not match from the journal-specific list. Please check, and correct if necessary.
Q5	Please check the author names in Ref. [8].
Q6	Please supply the year of publication for Ref. [20].
Q7	Please update Ref. [23].

<div style="border:1px solid black; display:inline-block; padding:8px;">
Please check this box if you have no corrections to make to the PDF file   ☐
</div>

Thank you for your assistance.

Uniaxially aligned electrospun fibers for advanced nanocomposites based on a model PVOH-epoxy system

Samaneh Karimi [a,*], Mark P. Staiger [b,c], Neil Bunk [d], Alison Fessard [e], Nick Tucker [f]

[a] The New Zealand Institute for Plant & Food Research, Lincoln 7608, New Zealand
[b] Department of Mechanical Engineering, University of Canterbury, Private Bag 4800, Christchurch 8140, New Zealand
[c] The MacDiarmid Institute for Advanced Materials and Nanotechnology, P.O. Box 600, Kelburn, Wellington 6140, New Zealand
[d] Electrospinz Limited, 44 Lee St, Blenheim 7201, New Zealand
[e] Department of Ergonomy, Design and Mechanical Engineering, Université de Technologie de Belfort Montbéliard, 90400 Sevenans, France
[f] School of Engineering, University of Lincoln, Brayford Pool, Lincoln LN6 7TS, United Kingdom

ARTICLE INFO

ABSTRACT

This work demonstrates the potential of aligned electrospun fibers as the sole reinforcement in nanocomposite materials. Poly(vinyl alcohol) and epoxy resin were selected as a model system and the effect of electrospun fiber loading on polymer properties was examined in conjunction with two manufacturing methods. A proprietary electrospinning technology for production of uniaxially aligned electrospun fiber arrays was used. A conventional wet lay-up fabrication method is compared against a novel, hybrid electrospinning–electrospraying approach. The structure and thermomechanical properties of resulting composite materials were examined using scanning electron microscopy, dynamic mechanical analysis, thermogravimetric analysis, differential scanning calorimetry, Fourier transform infrared spectroscopy, and tensile testing. The result demonstrate that using aligned electrospun fibers significantly enhances material properties compared to unreinforced resin, especially when manufactured using the hybrid electrospinning–electrospraying method. For example, tensile strength of such a material containing only 0.13 vol% of fiber was increased by ~700%, and Young's modulus by ~250%, with concomitant increase in ductility.

© 2015 Published by Elsevier Ltd.

1. Introduction

Electrospun fibers are highly drawn and so should exhibit a high degree of molecular order, thence approaching the theoretical maximum strength of the parent material. The draw ratio for a typical PVOH fiber measured as the ratio of diameters at the beginning of the spinning process (measured by light photographic image analysis), and the final drawn fiber size (measured by automated SEM image analysis) is about 100. It is expected that the process of fiber drawing from a polymer solution leads to a decrease in voidage, and an increase in tensile strength, tensile modulus and yield stress [1]. The effect has been specifically noted for PVA by Heikens et al. [2]. There is also readily observable empirical evidence, observed as fiber shrinkage associated with temperature increase. As a composite reinforcement, electrospun fibers will certainly exceed the critical fiber length over which the fiber itself must break if the composite article is to be broken. It is also known that

nano-scale fillers and extenders have a significant effect at low levels of addition. This paper therefore examines the use of low volume fractions of aligned electrospun fibers as the sole reinforcement in nano-composite materials. On a semantic note, the authors acknowledge that the electrospun fibers used are strictly sub-micron sized since their diameters are >100 nm, but they are small enough to be influencing the bulk properties of the composites by nanoscale interactions, and thus the product may be considered as a nanocomposite. This is evinced by the low percentage of fiber required to achieve a significant increase in macroscale properties.

The effects of nano-scale particulates, platelets and short fibers have been widely examined as thermoplastic polymer filler-extenders [3,4]. The significant effect of a low volume fraction of nanoscale materials is due to the formation of an interphase zone in the vicinity of the reinforcement surface where the dynamics of host polymer molecules are affected [5]. The high surface to volume ratio of these materials means that a significant volume fraction of the composite material is within this zone leading to a substantial effect on the mechanical properties of the manufactured article.

* Corresponding author.
   E-mail address: Samaneh.Karimi@plantandfood.co.nz (S. Karimi).

The conceptual step of manufacturing composite articles by following best practice for macro-scale advanced composites – long fibers in aligned arrays [6], has not been widely explored. This is perhaps because at the established macro-scale, to make composites with high levels of mechanical performance, high fractions of reinforcement in the composite are required. These high volume fractions may be difficult achieve with electrospun fibers due to the low rates of production achieved by wholly electrostatic processing. In addition, the ability to control the orientation of electrospun fibers when manufacturing in quantity is known, but not highly developed.

Electrospun fibers have been used as a component with macro-scale fibers to improve interlaminar shear properties of epoxy–carbon fiber composites [7], and as random oriented reinforcement improving the toughness of an epoxy resin, and the Young's modulus and tear strength of a styrene–butadiene rubber [8]. The need for highly aligned nano-fiber reinforcement has also been previously noted [9].

Numerous methods for the fabrication of aligned electrospun fibers have been described [10,11]. However, the mechanism for fabrication of aligned electrospun fibers is still an open problem, lacking much in theoretical analysis of the process, work by Liu et al. [12] being a notable exception. With electrospun fiber manufacture, the fiber production rate is typically low and collection and handling the fibers without distortion of alignment or damage is challenging.

The aligned fiber arrays used in the work described in this paper are made using a proprietary technology, developed from a proposal by Nurfaizey et al. [13] which addresses the twin difficulties of control of production rate and fiber handling. The method uses a hybrid approach combining gap spinning with synchronized variation in the electrostatic field which allows the deposition of a controlled number of highly aligned fibers. There have been previous attempts at producing stacked arrays of oriented fiber. Li et al. [14] used a gap spinning method coupled with sequential earthing of a radial electrode array to produce multi-layer stacks of controlled orientation fibers. However, no method of scale up, or proposal for a technique to remove the fiber from the collector substrate is given.

Materials were selected based on processability and successful use in the manufacture of macro scale composites [15], poly(vinyl alcohol) being chosen for the fiber, and epoxy resin for the matrix. Two different composite manufacturing methods were explored:

(i) Conventional wet lay-up followed by vacuum consolidation.
(ii) Deposition of the uncured epoxy matrix into the reinforcement layer-by-layer using electrospraying, followed by vacuum consolidation.

These methods were chosen to minimize disturbance to the fiber layup pattern by fiber wash. The different approaches to processing were expected to result in different degrees of fiber-resin interaction, and thence differing mechanical properties in the final composite materials. The morphology, chemical structure and thermo-mechanical properties of fabricated materials were studied and analyzed as described below.

2. Experimental procedures

2.1. Materials

The poly(vinyl alcohol) (PVOH) used as reinforcement was supplied as pellets (Mw = 118,000–124,000 g/mol, DH = 86–89, Chemiplas NZ limited, New Zealand). The pellets were dissolved in distilled water by stirring at 60 °C for 2 h. The final PVOH concentration of the aqueous solution was adjusted to 8 wt%. The epoxy resin and hardener (West System 105 resin, West System 206 hardener, Nuplex Ltd., New Zealand.) were mixed in the mass ratio of 5:1 for use as the matrix polymer.

2.2. Production of uniaxially aligned fibers

The electrospinning process was carried out using a proprietary gap spinning and field control method. Aligned PVOH fibers were made using an applied voltage of 12 kV and a nozzle-to-collector distance of 160 mm to produce mats with nominal dimensions of 96×60 mm ($l \times w$). The mats were collected after deposition times of 30, 60 and 90 min on a stainless steel plate covered with silicone release paper. All electrospun materials were dried in a vacuum oven at 50 °C overnight prior to further measurements.

Attempts were made to weigh the mats using a four figure microbalance (Mettler Toledo AE 166) to quantify the rate of fiber production. However, the microbalance readings were unstable even with the use the Ionizer Antistatic System (Mettler Toledo) designed to remove surface charge build-up from specimens. This is because the transient imbalance in the number of electrons on the surface of the fibers is not the only way that electrospun fibers retain charge. It is known that electrospun fibers retain charge for periods of years [16,17]. This more persistent charge is due to the change of state of the polymer from liquid to solid whilst inside a strong electrical field, leading to the formation of a stable electric charge held within the fiber (an electret) as a result of dipole polarization [18]. It is the presence of this internal charge that leads to the difficulties in weighing small samples of electrospun fibers – the effect of this phenomenon on electrospinning is the subject of on-going research to be described in a future publication. Therefore, an alternative method of estimating the volume of electrospun fiber by image analysis of scanning electron micrographs was used. The spinning method gives a high degree of control of the thread count of the finished product, and this was exploited to measure the fiber volume of the finished composites. The numbers of fibers per mm of width of electrospun mat were counted and the results were used in conjunction with fiber diameter measurements to create a calibration curve that was then used to estimate the volume of electrospun fiber in the finished composite (Fig. 1).

2.3. Preparation of nanocomposites using the wet lay-up method

A single layer of electrospun mat was placed onto silicone release paper. 0.2 g of pre-mixed epoxy resin and hardener was poured onto the top surface of the mat, allowing the resin to fully impregnate the mat and form a thin film. The surface of the film was then covered with another sheet of silicone release paper. The film was then
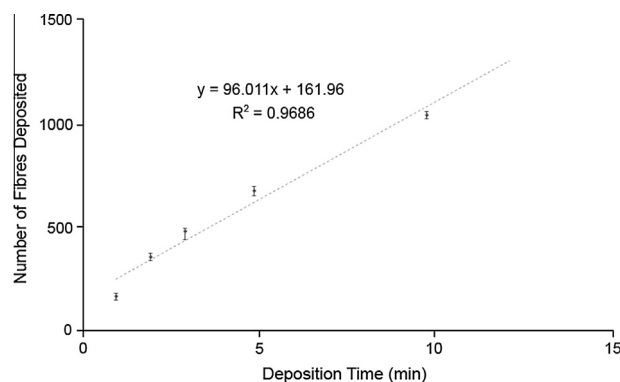

Fig. 1. Number of electrospun fibers per mm of mat width as a function of deposition time.

loaded onto a stainless steel support plate, placed inside a 280 × 400 mm metallized foil pouch (3 seal silver foil pouch, Cas-Pak Products Ltd., New Zealand), evacuated and sealed using an A300/16 Multivac vacuum sealer (Sepp Haggenmüller GmbH & Co, Germany) prior to being subjected to a curing cycle of 45 °C for 24 h. Films made by this method were labeled WL (wet lay-up) along with the fiber deposition time in minutes (e.g. WL30).

2.4. Preparation of nanocomposites using the hybrid electrospinning-electrospraying method

An electrospinning machine (Model ES1, Electrospinz Ltd., New Zealand) was used to electrospray epoxy resin onto the electrospun mat using an applied voltage of 12 kV.

The plate holding the electrospun fiber mat was installed on a moving rail to give a set distance from the spraying tip (15 cm) and the plate was moved through the field of spray at constant rate three times. This deposited the same amount of epoxy/hardener mixture that was used in the wet lay-up approach (0.2 g). Then similarly to the wet lay-up approach, the film was loaded onto a stainless steel support plate, vacuumed, sealed and cured at 45 °C for 24 h. Films made through this processing technique were labeled as HEE (hybrid electrospinning-electrospraying) along with the fiber deposition time in minutes (e.g. HEE30). A schematic of the hybrid process is presented in Fig. 2.

Using the calibration curve (Fig. 1) 30, 60 and 90 min of fiber deposition gave 0.045, 0.09 and 0.13 vol% of fibers in the used amount of matrix. All of the fabricated films maintained a similar range of final thickness of 0.1 ± 0.02 mm. Specimens were conditioned at a nominal temperature of 20 ± 1 °C and relative humidity of 35 ± 1% for 4 days prior to testing.

Various treatments and their associated labels are summarized in Table 1.

2.5. Materials characterization

The surface morphology, diameter and alignment of the electrospun fibers, and fracture surfaces of the thin films were examined by scanning electron microscopy (SEM) (JEOL Neoscope JCM-5000, USA). Specimens were sputter-coated with gold for 240 s (Quorum Q150R sputter coater, Quorum Technologies Ltd., UK). The average diameter of the PVOH fiber was based on the measurement of ~200 fibers by computer image analysis of scanning electron micrographs (Electrospinz SEM Analyser software, Electrospinz Ltd., New Zealand) [19].

The tensile properties of the nanocomposite materials were measured using a universal testing machine (Instron 4444) equipped with a 0.5 kN load cell. Rectangular coupons (80 (l) × 6 (w) × 0.1 (t) mm) were tested at room temperature using a gauge length of 25 mm in accordance with ASTM D882 using a crosshead speed of 50 mm/min. The quoted Young's modulus, ultimate tensile strength and elongation at break of each composite material were averaged from at least 4 replicates. A pair of 3D printed dumb bell-shaped tensile specimens were also prepared from polylactide (Maker Gear 3D printer, MakerGear LLC, USA) to provide a non-slip gripping surface during the testing of the composite films (Fig. 3). The middle gauge section of the dumb bells was removed and a coupon of the composite film was then sandwiched between the two dumb bells for tensile testing. This method reliably produced a breakage point in the middle of the specimen.

Dynamic mechanical analysis (DMA) is a commonly ascribed method of estimating the glass transition point [20]. DMA was carried out within the linear viscoelastic range of the samples by means of a TA Instruments Q800 machine (TA Instruments, USA) in tensile mode using rectangular specimens (15 (l) × 5 (w) × 0.1 (t) mm). The storage (E′) and loss (E″) moduli were measured at a
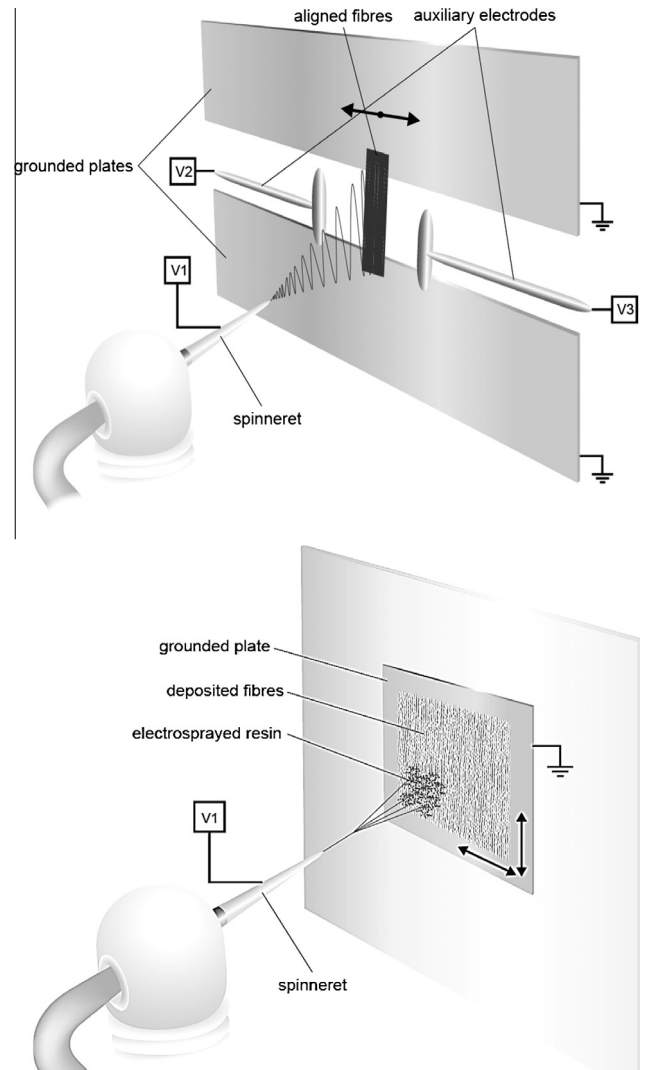

Fig. 2. Schematic of the electrospinning process (top) and the electrospraying process (bottom).

Table 1
Treatments guide.

Deposition time (min)	Fiber loading (vol%)	Processing method	
		Wet lay-up	Hybrid electrospinning-electrospraying
0	0	URE (unreinforced epoxy)	
30	0.045	WL30	HEE30
60	0.090	WL60	HEE60
90	0.130	WL90	HEE90

frequency of 1 Hz over a temperature range of 20 to 150 °C. The temperature ramp rate was 5 °C/min.

Thermogravimetric analysis (TGA) was carried out using a TA Instruments Q600 (TA Instruments, USA). Specimens (~3 mg) were placed in platinum pans and heated from 20 to 500 °C at a heating rate of 10 °C/min under a nitrogen atmosphere.

Differential scanning calorimetry (DSC) was performed using a TA Instruments Q2000 (TA Instruments, USA) equipped with a refrigerated cooling system (RCS90). Specimens (~1.5 mg) were cut to lay flat on the base of the low mass Tzero aluminum pan. To remove any effects of prior thermal history, specimens were first heated for 10 min, cooled, and then reheated over a temperature range of 20–250 °C at a heating rate of 10 °C/min.
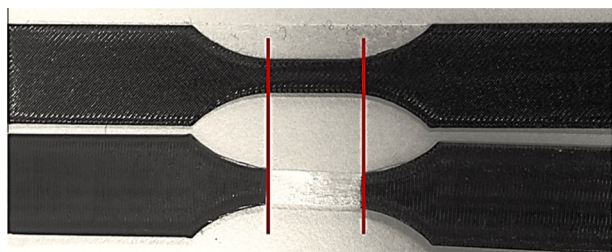
Fig. 3. Photograph of tensile sample preparation: 3D printed specimen (top), and one of the fabricated samples sandwiched between the two printed specimens (bottom). (For interpretation of the references to color in this figure legend, the reader is referred to the web version of this article.)

Fourier transform infrared spectroscopy (FT-IR) was carried out on the electrospun mat, the unreinforced epoxy resin and the product nanocomposites using a Bruker ALPHA series spectrometer (Bruker Optics GmbH, Germany) equipped with an ALPHA platinum ATR single-reflection diamond ATR module. Samples were placed directly on the ATR plate for measurements. Spectra were averaged over 16 scans using a resolution of $2\,cm^{-1}$ over the mid-IR range (4000–$400\,cm^{-1}$). The data was analyzed using OPUS software (Bruker).

3. Results and discussion

3.1. Microstructural analysis

The average diameter of the uniaxially aligned PVOH fibers was 267 nm, (Fig. 4a-b). SEM image analysis also revealed that almost 96% of fibers are uniaxially aligned. The distribution of fiber diameters is depicted in Fig. 4c.

The unreinforced epoxy films exhibited brittle fracture, this being denoted by the presence of smooth fracture surfaces (Fig. 5a). The presence of epoxy beads on the broken fibers at the fracture surface of the wet layup films implies significant interfacial adhesion between the two phases (Fig. 5b). This is attributed to a degree of fiber/matrix compatibility and the possible presence of hydrogen bonding interactions existing at the PVOH-epoxy interface. Chihani et al. [21] have observed that PVOH is retained at the surface of an epoxy resin following washing with hot water, indicating that PVOH may form a bond with epoxy resin via its hydroxyl groups. Peijs et al. investigated the mechanical properties of composites based on conventional scale solution spun PVOH fibers and epoxy resin and showed that, in general, their structural performance is between those of plasma-treated High Density Polyethylene (HDPE) and aramid fiber-reinforced composites, due to the combination of a strong interfacial bond strength and fibers with isotropy [22].
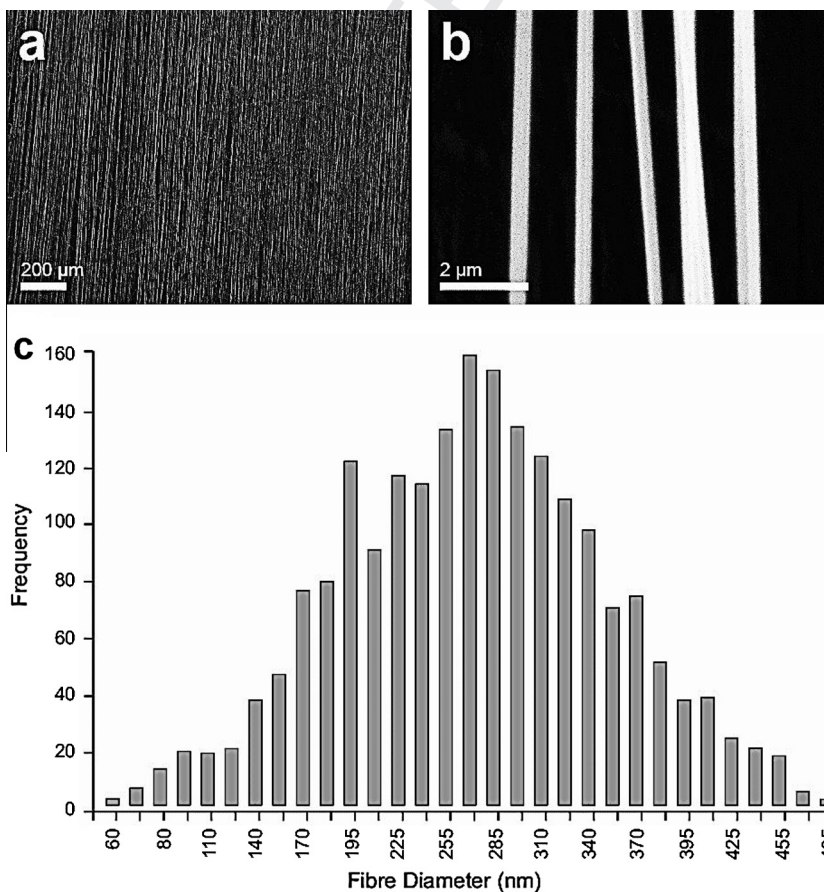
The hybrid electrospin/spray films revealed considerably different fractographic features (Fig. 5c), implying an enhancement in the level of the fiber/matrix interaction resulting from the application of the electrosprayed resin. Electrospraying produces a fine atomized spray, as the formation of droplets is not just the result of the action of surface tension, but there may also be an element of electrostatic influence leading to Rayleigh scattering of the droplets. The rough fracture surface and indistinct epoxy/fiber interface qualitatively indicate an enhanced interfacial interaction of the two phases. The reinforced epoxy exhibited a ductile fracture surface, implying that the addition of fibers was effective in reducing the brittleness inherent in an epoxy matrix.

Fig. 4. (a and b) Scanning electron micrographs of electrospun fibers and (c) aligned fibers diameter distribution.
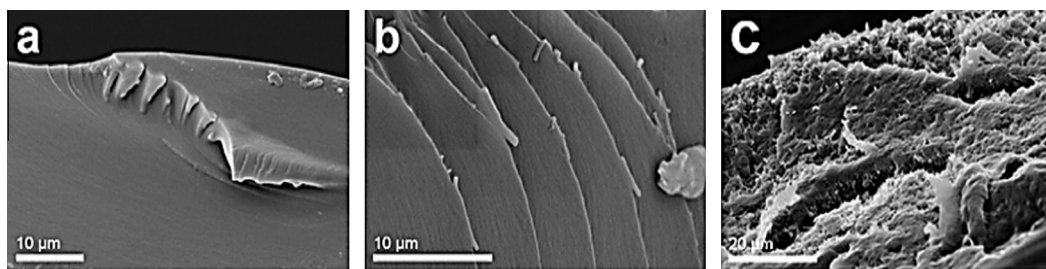
Fig. 5. SEM of the tensile fracture surfaces of (a) URE, (b) WL90, and (c) HEE90.

Additional SEM micrographs is provided in the related Data in Brief paper [23].

3.2. Tensile properties

The tensile strength, Young's modulus and elongation at break all showed significant and progressive enhancement proportional to the level of fiber loading for both types of nanocomposites (Fig. 6). Engineering stress–strain curves and additional data can be found in the related data in Brief paper [23].

Significant increases in tensile strength (472%), Young's modulus (234%) and elongation at break (278%) against unreinforced matrix, were recorded for WL90. Changing the processing tech-nique to the hybrid electrospun/spraying method lifted these values to a tensile strength of 695%, Young's modulus of 246% and elongation of break of 286% (data from HEE90). In the case of the conventionally manufactured wet layup samples, it is proposed that the electrospun fibers bridge across cracks that develop in the epoxy matrix, thereby contributing to a redistribution of stresses where damage mechanisms are initiated (e.g. interfacial debonding). This has the effect of delaying failure, resulting in the observed elevation in mechanical performance of the reinforced epoxy.

The significant contrast in results of the hybrid electrospin/spray versus wet layup films suggests that this novel hybrid processing approach increases the fiber/matrix interfacial contact area. This should improve the efficiency of interfacial interaction and encourage the formation of a 3D fiber/matrix network, securing a percolation electrospun fiber network within the matrix, although further work is needed to confirm this.

The improved stiffness and ductility is a departure from the usually observed properties of nanocomposites, when increases in modulus occur at the expense of elongation at break [24–26]. The improved ductility, observed as an increase of elongation in break is due to fiber related delocalization of strain.

The alignment of electrospun fibers is a noteworthy feature which is likely to have led to this significant enhancement in mechanical properties as aligned fiber arrays are classically more efficient reinforcements than randomly orientated fibers. For example, the tensile strength in the longitudinal direction is increased seven fold compared to that of a random mat in a study of epoxy reinforced with an aligned electrospun cellulose nanofibrous mat [27].

3.3. Dynamic mechanical analysis

The temperature dependence of the dynamic mechanical behavior of the materials is depicted in Fig. 7. The unreinforced epoxy resin exhibited a more rapid decrease in the storage modulus (E') with temperature as compared to the composites (Fig. 7).

The glass transition temperature (T_g) of the unreinforced epoxy was increased by the presence of PVOH fibers from 68 °C to a value in the range of 71–92 °C, indicating a strong interaction between the PVOH fibers and epoxy matrix. Overall, the PVOH-reinforced epoxy showed an increased E' over the investigated temperature range and the greatest increase was observed in the HEE90 film (Fig 7).

The storage modulus of WL90 and HEE90 films at 75 °C was increased by 28 and 38 fold over that of the unreinforced matrix; these are significant results considering the low volume fraction of the reinforcing phase (PVOH). Miyagawa et al. investigated the thermophysical properties of epoxy nanocomposites reinforced by two types of carbon nanotubes (CNT) prepared by a sonication method [28]. They reported a decrease in glass transition temperature and decomposition temperature of nanocomposites with increasing amount of CNT. Only when they modified their
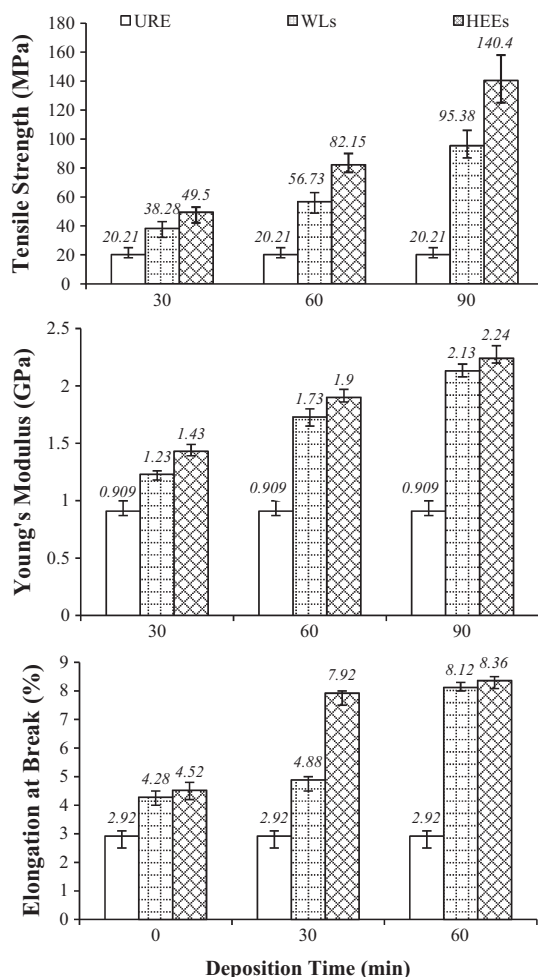

Fig. 6. Tensile strength (MPa), Young's Modulus (GPa) and Elongation at break (%) of fabricated materials with varying fiber content.
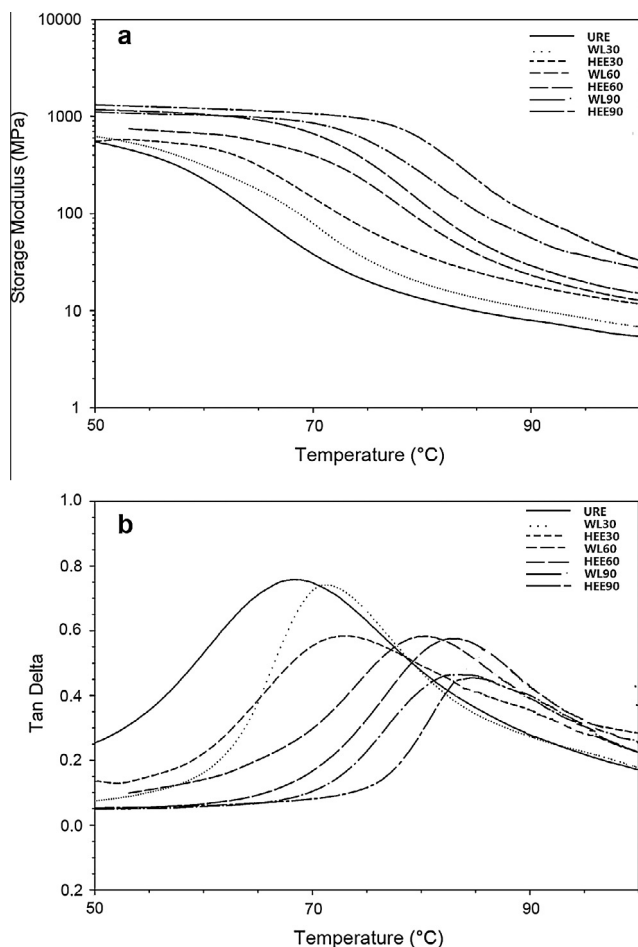
6   S. Karimi et al./Composites: Part A xxx (2015) xxx–xxx

Fig. 7. (a) The storage modulus (E′) and (b) tanδ curves as a function of temperature.

Fig. 8. (a) TG and (b) DTG curves of studied materials.

manufacturing process, did they achieve a 20% boost in storage modulus of CNT/epoxy nanocomposites at a level of nanotube incorporation of 0.21 vol%.

According to obtained data, with increasing fiber content, the tanδ peak shifted toward higher temperatures. Typically the higher the T_g, the higher the cross-linked density and the higher the modulus. As expected, the most prominent temperature peak shift occurred in the HEE90 which was +24 °C. The height of tan δ peaks decreased for the fiber/epoxy nanocomposite films, suggesting that the dampening effect was reduced by fibers embedded in the matrix. The significant reinforcing effect observed in the hybrid electrospin/spray material is ascribed to the intimacy of the fiber/epoxy interfaces which allow the fibers to efficiently communicate loads through the matrix via the percolation network held by hydrogen bonds, thus reducing the effect of force impact and deformation and thereby enhancing the storage modulus above T_g.

3.4. Thermogravimetric analysis

To help to understand the nature of the interactions between the constituent phases and to examine the effect of manufacturing methods and fiber loading on the thermal stability of fabricated films, TGA experiments were carried out and main data are summarized in the related Data in Breif paper [23]. The PVOH electrospun fiber mats had the lowest thermal stability of the studied materials (onset of degradation at 268 °C) with a three-stage thermal decomposition process. The first stage presents the loss of weak physically absorbed water from the fibers and second stage
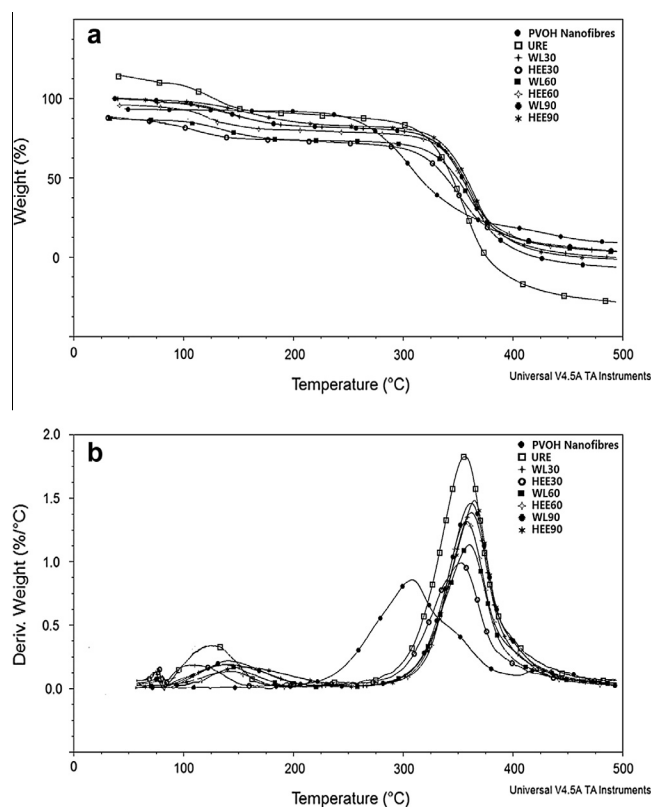
exhibits the decomposition of the PVOH side chains. The third stage shows the decomposition of the main chain structure of the PVOH [29] with the recorded T_{max} of 308 °C. Based on the DTG profile, thermal degradation of epoxy was a two-step process. In the first stage, which involves a mass loss of 13.24%, is for drying and loss of volatile compounds (at 125 °C). The second stage is thermal decomposition of epoxy with onset temperature of 326 °C resulting in a mass loss of 42% and continuing to a significant mass loss of about 69% or 83% of the total mass of original sample at 355 °C.

The thermal degradation profile of these materials when combined into nanocomposite films showed similar effects. HEE90 film presented the most prominent T_{max} shift of +9 °C (Fig. 8). This observation reinforces the arguments proposed in the previous section.

3.5. Differential scanning calorimetry

The DSC analysis of the PVOH electrospun fiber mats revealed an endothermic melting peak at ∼192 °C with an enthalpy of fusion of 35 J/g. The complete disappearance of this peak after the first heating run in all of the nanocomposite films is evidence of efficient fiber/matrix interaction (Fig. 9a). Superimposing the DSC thermograms of second heating run (thus removing the thermal history of the samples) on the nanocomposites made by the two different techniques allowing comparison with the unreinforced epoxy film, revealed a smooth progressive T_g shift, similar to that revealed by the DMA observations (Fig. 9b).

Overall, all three thermal analysis techniques (DMA, TGA and DSC) produced consistent results indicating a general increase in the thermal stability of the fabricated composite materials associated with the level of electrospun fiber addition, and demonstrated the superiority of nanocomposites made by the hybrid electrospinning–electrospraying approach.

3.6. Fourier transform infrared spectroscopy

The mid-IR spectrum of unreinforced epoxy exhibited several bands characteristic of bending and stretching vibrations of O—H, C—H, C—C, C=C and C—O groups (Fig. 10). An expanded short peak observed around 3500 cm^{-1} in the unreinforced epoxy spectrum corresponds to the presence of the hydroxyl groups. In this range, the addition of PVOH electrospun fibers induces a greater peak, due to the presence of O—H groups in PVOH electrospun fibers. The strong and noticeably expanded peak around 2900 cm^{-1} is assigned to the C—H groups of the aromatic rings of unreinforced epoxy. The addition of PVOH electrospun fibers to the epoxy matrix produces a higher peak, due to the multitude of C—H bonds in the structure of the PVOH polymer. At 1600 cm^{-1}, a peak which corresponds to the C—C bond of epoxy molecule is observed, and is greater in magnitude in the nanocomposite samples. This is related to absorbance of C—C bond which is higher for the nanocomposites, as the PVOH molecule is mainly created by C—C liaisons (shown by the high peak at 1700 cm^{-1} for the PVOH sample).

The strong double peak at 1500 cm^{-1} is assigned to the C=C vibration in the aromatic rings of unreinforced epoxy. The addition of the PVOH electrospun fibers has only a slight effect on the intensity of the peak, as there is no C=C vibration in PVOH polymer. Observing the spectrum of unreinforced epoxy in the range 1250–800 cm^{-1}, the bands are assigned to the C—O bonds between the aromatic rings and O—H groups. The addition of the PVOH electrospun fibers has a great effect on the intensity of the peak, because the C—O stretching in PVOH electrospun fibers is very high (as shown by the peaks at 1250 cm^{-1} and around 1000 cm^{-1}).
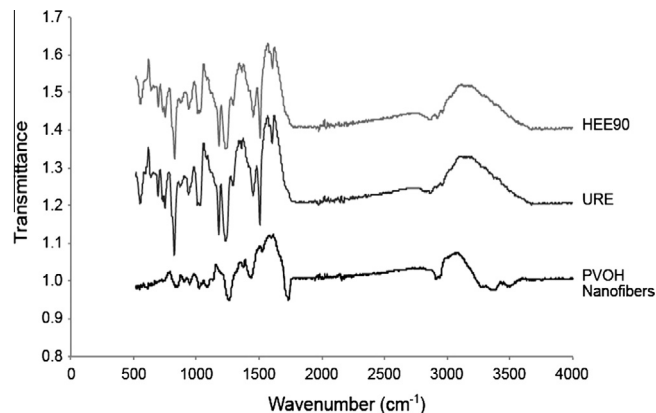

Fig. 10. Superposition of FTIR spectra.

The main peaks of the nanocomposites samples can be observed at higher wave numbers than those of the unreinforced epoxy. It is also significant that the general absorbance is generally higher for the nanocomposites than for unreinforced epoxy, and that the absorbance increases with the proportion of electrospun fibers in the sample. These findings could be evidence of chemical bonding and interfacial interactions between the electrospun fibers and the epoxy matrix.

3.7. Optical transparency

The unreinforced epoxy resin is optically transparent and the addition of electrospun fibers did not cause any visual change in the transparency of the final product. In most cases the light transmittance is decreased by the addition of fibers to composite films unless the refractive index of the fibers and the matrix match. All of the nanocomposite films made in this work exhibited high light transmittance in the visible light region regardless of fiber content or processing approach (Fig. 11). This high level of transparency is attributable to minimal light scattering due to the small diameter of the reinforcing fibers (~267 nm) that is below the wavelength of visible light (380–750 nm) [30,31].
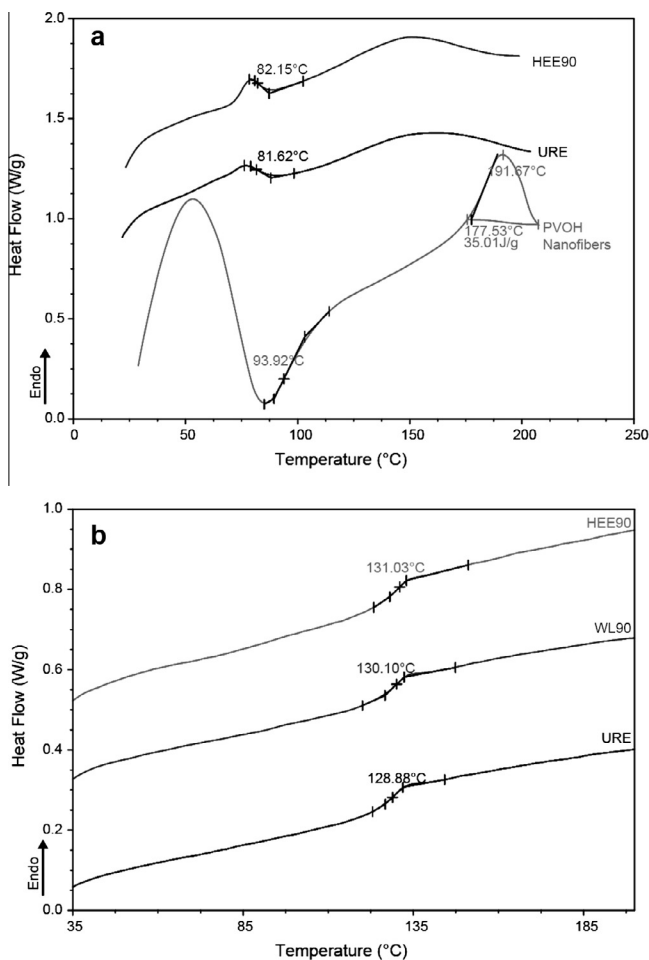

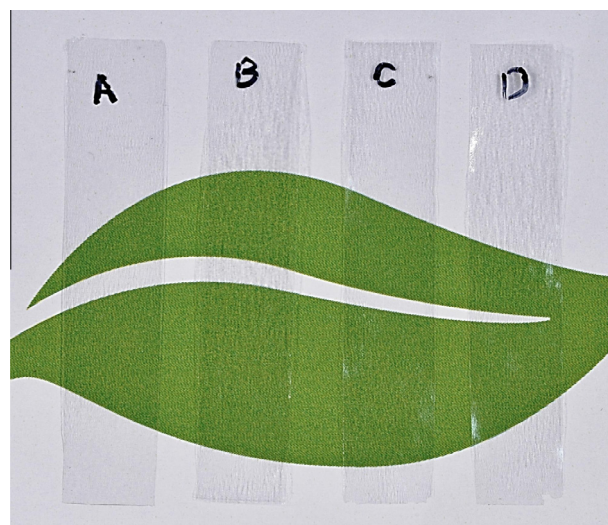**Fig. 9.** DSC graphs of (a) first and (b) second heating runs.

Fig. 11. A photograph of fabricated films demonstrating optical transparency: (A) URE, (B) HEE30, (C) WL90, (D) HEE90. (For interpretation of the references to color in this figure legend, the reader is referred to the web version of this article.)

4. Conclusions

This research demonstrates that by using uniaxially aligned electrospun fibers, it is possible to make a considerable shift in thermal and mechanical performance of nanocomposite materials whilst simultaneously increasing the modulus and elongation at break, a rare combination that has not been demonstrated with traditional nanoscale short fibers or carbon nanotubes. The significant increase in mechanical properties at low levels of fiber addition indicates that the presence of aligned electrospun fibers made by electrospinning, with evident good interfacial adhesion between matrix and filler, are efficient reinforcements for composite articles. The novel hybrid electrospinning-electrospraying processing approach, further improved the properties of the nanocomposites, and is a robust manufacturing method with a ready potential for scale-up to automated processing. It is worth noting that conventional injection based composite manufacturing techniques may not be suitable for use with electrospun fibers due to the combined risk of fiber wash and poor impregnation. Electrospraying protects the electrospun fibers from handling damage, and importantly does not affect fiber alignment.

Acknowledgements

References

[1] Ziabicki A. Fundamentals of fibre formation: the science of fibre spinning and drawing. John Wiley & Sons; 1976.
[2] Heikens D, Bleijenberg A, Hoppenbrouwers J, Barentsen W. The influence of stretching on tensile strength and solubility of poly (vinyl alcohol) fibres. Polymer 1971;12(12):797–801.
[3] Paul DR, Robeson LM. Polym Nanotechnol: Nanocompos Polym Compos 2008;49:17.
[4] Ajayan PM, Schadler LS, Braun PV. Nanocomposite science and technology. Wiley & Sons; 2006.
[5] Hua L, Brinson C. Reinforcing efficiency of nanoparticles: a simple comparison for polymer nanocomposites. Compos Sci Technol 2007;68:10.
[6] Kelly A. Concise encyclopedia of composite materials. Oxford: Pergamon Press; 1989.
[7] Dzenis Y, Reneker DH. Delamination resistant composites prepared by small diameter fiber reinforcement at ply interfaces. USA: Board of Regents, University of Nebraska-Lincoln; 2001.
[8] Jong-Sang Kim, Reneker DH. Mechanical properties of composites using ultrafine electrospun fibers. Polym Compos 1999;20(1):124–31.
[9] Windle AH. Two defining moments: a personal view by Prof. Alan H. Windle. Compos Sci Technol 2007;67(5):929–30.
[10] Long Y-Z, Sun B, Zhang H-D, Duvail J-L, Gu C-Z, Yin H-L. Fabrication and applications of aligned nanofibers by electrospinning. Nanotechnol Res J 2014;7(2):155.
[11] Teo W, Ramakrishna S. A review on electrospinning design and nanofibre assemblies. Nanotechnology 2006;17(14):R89.
[12] Liu H-Y, Ji-Huan He D, Kong H, David Ho J. Highly aligned electrospun nanofibers/nanoporous fibers: numerical analysis and experimental verification. Int J Numer Meth Heat Fluid Flow 2014;24(6):1321–30.
[13] Nurfaizey A, Stanger J, Tucker N, Buunk N, Wallace A, Staiger M. Manipulation of electrospun fibres in flight: the principle of superposition of electric fields as a control method. J Mater Sci 2012;47(3):1156–63.
[14] Li D, Wang Y, Xia Y. Electrospinning nanofibers as uniaxially aligned arrays and layer-by-layer stacked films. Adv Mater 2004;16(4):361–6.
[15] Peijs T, Van Vught R, Govaert L. Mechanical properties of poly (vinyl alcohol) fibres and composites. Compos Sci Technol 1995;50(8):7.
[16] Filatov Y, Budyka A, Kirichenko V. Electrospinning of micro-and nanofibers: fundamentals in separation and filtration processes. J Eng Fibers Fabrics 2007;3:488.
[17] Kliemann B, Stoll M. Process and apparatus for the preparation of electret filaments, textile fibers and similar articles. Google Pat 1984.
[18] Cross J. Electrostatics: principles, problems and applications; 1987.
[19] Stanger J, Tucker N, Buunk N, Truong Y. A comparison of automated and manual techniques for measurement of electrospun fibre diameter. Polym Testing 2014;40:4–12.
[20] Roe R. Glass transition. In: Kroschwitz J, editor. Concise encyclopedia of polymer science and engineering. John Wiley and Sons. p. 434. **Q6**
[21] Chihani T, Flodin P, Hjertberg T. Modification of epoxy surfaces with different polyvinylalcohol polymers. J Appl Polym Sci 1993;50(8):1343–50.
[22] Peijs T, Van Vught R, Govaert L. Mechanical properties of poly (vinyl alcohol) fibres and composites. Composites 1995;26(2):83–90.
[23] Karimi S, Staiger MP, Buunk N, Fessard A, Tucker N. Complementary characterization data in support of uniaxially aligned electrospun **Q7** nanocomposites based on a model PVOH-epoxy system. Data in Brief; 2015 (submitted for publication).
[24] Marras SI, Kladi KP, Tsivintzelis I, Zuburtikudis I, Panayiotou C. Biodegradable polymer nanocomposites: the role of nanoclays on the thermomechanical characteristics and the electrospun fibrous structure. Acta Biomater 2008;4 (3):756–65.
[25] Causin V, Yang B-X, Marega C, Goh SH, Marigo A. Nucleation, structure and lamellar morphology of isotactic polypropylene filled with polypropylene-grafted multiwalled carbon nanotubes. Eur Polymer J 2009;45(8):2155–63.
[26] Karimi S, Tahir PM, Dufresne A, Karimi A, Abdulkhani A. A comparative study on characteristics of nanocellulose reinforced thermoplastic starch biofilms prepared with different techniques. Nord Pulp Pap Res J 2014;29(1):41–5.
[27] Liao H, Wu Y, Wu M, Zhan X, Liu H. Aligned electrospun cellulose fibers reinforced epoxy resin composite films with high visible light transmittance. Cellulose 2012;19(1):111–9.
[28] Miyagawa H, Rich MJ, Drzal LT. Thermo-physical properties of epoxy nanocomposites reinforced by carbon nanotubes and vapor grown carbon fibers. Thermochim Acta 2006;442(1):67–73.
[29] Othman N, Azahari NA, Ismail H. Thermal properties of polyvinyl alcohol (PVOH)/corn starch blend film. Malaysian Polym J 2011;6(6):147–54.
[30] Yano H, Sugiyama J, Nakagaito AN, Nogi M, Matsuura T, Hikita M, et al. Optically transparent composites reinforced with networks of bacterial nanofibers. Adv Mater 2005;17(2):153–5.
[31] Ifuku S, Morooka S, Morimoto M, Saimoto H. Acetylation of chitin nanofibers and their transparent nanocomposite films. Biomacromolecules 2010;11 (5):1326–30.